Optics & Laser Technology 70 (2015) 63–70

Contents lists available at ScienceDirect

Optics & Laser Technology

journal homepage: www.elsevier.com/locate/optlastec

# Automatic detection of zebra crossings from mobile LiDAR data

B. Riveiro [a], H. González-Jorge [b,*], J. Martínez-Sánchez [b], L. Díaz-Vilariño [b], P. Arias [b]

[a] Applied Geotechnology Group, School of Industrial Engineering, University of Vigo, Rúa Máxwell s/n, Campus Lagoas Marcosende, 36310 Vigo, Spain
[b] Applied Geotechnology Group, School of Mining Engineering, University of Vigo, Rúa Maxwell s/n, Campus Lagoas-Marcosende, 36310 Vigo, Spain

ARTICLE INFO

*Article history:*
Received 22 November 2014
Received in revised form
22 December 2014
Accepted 26 January 2015
Available online 13 February 2015

*Keywords:*
Urban mapping
Mobile LiDAR
Geographic information system

ABSTRACT

An algorithm for the automatic detection of zebra crossings from mobile LiDAR data is developed and tested to be applied for road management purposes. The algorithm consists of several subsequent processes starting with road segmentation by performing a curvature analysis for each laser cycle. Then, intensity images are created from the point cloud using rasterization techniques, in order to detect zebra crossing using the Standard Hough Transform and logical constrains. To optimize the results, image processing algorithms are applied to the intensity images from the point cloud. These algorithms include binarization to separate the painting area from the rest of the pavement, median filtering to avoid noisy points, and mathematical morphology to fill the gaps between the pixels in the border of white marks. Once the road marking is detected, its position is calculated. This information is valuable for inventorying purposes of road managers that use Geographic Information Systems.

The performance of the algorithm has been evaluated over several mobile LiDAR strips accounting for a total of 30 zebra crossings. That test showed a completeness of 83%. Non-detected marks mainly come from painting deterioration of the zebra crossing or by occlusions in the point cloud produced by other vehicles on the road.

## 1. Introduction

Cities are increasingly large and complex areas that require integrated technologies for an effective management and to ensure productivity, continued economic growth and environmental sustainability. The city management is increasingly supported by information technologies, leading to paradigms such as smart cities, where decision-makers, companies, and citizens are continuously interconnected. One of the computational tools that support smart cities management is the Geographic Information Systems (GIS). They organize information in layers with georeferenced data relevant to the city management. Typical GIS layers for urban management consist of urban elements such as horizontal and vertical signs, bus shelters, rubbish containers, lamps, banks, gardens, fountains, etc.

One of the most used spatial data acquisition technologies comprises the mobile LiDAR systems that achieve geo-reference point clouds and imagery in an accurate and productive manner. Mobile LiDAR systems acquire massive information, which must be organized in order to extract data of interest for geospatial analysis [1–3]. For example, a point cloud with several thousands of 3D points that describe the geometry of a traffic light is not very useful, although its geographic position of the urban object, height, manufacturer, type of luminaire, and maintenance events are aspects of interest for the infrastructure manager. Then, it can be affirmed that the users of LiDAR data more and more demand the development of algorithms to automatically extract useful information from large point clouds. This fact is corroborated by the intense work reported in the literature in recent years about automatic detection and classification of urban objects from LiDAR data.

Jaakkola et al. [4] develop algorithms for the detection of road curbstones using gradients in height plane. Hernández and Marcotegui [5] developed a methodology for the segmentation of the pavement contour using a quasi-flat zone algorithm. Pu et al. [6] present a framework for structure recognition from mobile laser scanner point cloud. It performs a rough classification of elements into three main categories (ground surface, objects on ground, and objects off ground). Using characteristics from the point cloud like size, shape, orientation and topological relationships, objects on ground are more detailed classified in signs, trees, building walls, and barriers. Mc. Ehinney et al. [7] design an algorithm for extracting the road edge using LiDAR and navigation data. Kumar et al. [8] developed an algorithm for extracting road edges using mobile LiDAR data. The algorithm is based on the snake model. It uses parameters selected empirically and fixed for all the road sections. The snake model is initialized based on the navigation information from the navigation system. Puente et al. [9] detect luminaires on a road tunnel using the RGB images registered over the point cloud of the tunnel. They perform an automated inventory in a productive and robust manner.

[*] Corresponding author. Tel.: +34 986818752.
*E-mail address:* higiniog@uvigo.es (H. González-Jorge).

http://dx.doi.org/10.1016/j.optlastec.2015.01.011
0030-3992/© 2015 Elsevier Ltd. All rights reserved.

Wang et al. [10] estimate the excavation volume in road widening from mobile LiDAR data. Normals of the points and slopes are used to separate road from off-road points. The left and right sides of the road points are sliced up to a distance of 4 m perpendicular to the roadside. Summing each sliced volume permits the calculation of the required excavation for a road widening. Cabo et al. [11] show an algorithm for the automatic extraction of pole-like street furniture objects. The method simplifies the point cloud based on space voxelization. The horizontal sections are then analized to detect the circular shape pattern of the poles. González-Jorge et al. [12] exhibit an automated method for the detection of surface efflorescence in road overpasses. They detect the overpasses using geometrical considerations and extract information from the efflorescence using the radiometric information from the LiDAR. Holgado-Barco et al. [13] use mobile LiDAR data and computational algorithms to extract geometric parameters from the road (vertical profiles and cross-sections) to characterize the proper construction and road safety assessment.

Although there was a huge activity during last years for the automatic detection of road elements from mobile LiDAR data, unresolved situations still remain. One example is the automatic inventory of zebra crossing from mobile LiDAR data. Some successful attempts using image processing for the detection of zebra crossings have been done, although an accurate geo-positioning of the elements cannot be achieved [14–16]. Direct detection of zebra crossing from mobile LiDAR data with the corresponding geo-positioning information is not found in the bibliography. Zebra crossing is repetitive element in urban roads and their inventory and inspection are especially important for road safety. The manuscript is organized in the following form: Section 2 presents the study cases where the algorithm was validated and the LiDAR system used for data acquisition and the methodology used for automatic data management. Section 3 shows the results and discussion and finally the conclusions are presented in Section 4.

## 2. Materials and methods

### 2.1. Study cases

Three mobile LiDAR datasets were used for this work. The mobile LiDAR survey was done without interrupting the traffic conditions using the Optech Lynx mobile mapper from the University of Vigo. In all cases the dilution of precision of the global navigation satellite system (GNSS) was kept below 2.5 to obtain accurate data. The surveying vehicle acquires 5 min of GNSS data before and after each strip to guarantee the maximum quality in the GNSS post-processing calculation. The acquisition frequency of the inertial measurement unit (IMU) of the Optech was configured to 200 Hz to acquire an accurate trajectory data. PosPAC software developed by Applanix (a Trimble company) is used to link the GNSS with the IMU data. It uses forwards and backwards navigation solution based on Kalman filtering. LiDAR sensors were set up at 500 kHz (laser measurement rate) and 200 Hz (scan frequency) to provide a dense point cloud, with the maximum possible resolution. LiDAR data are combined with the navigation data provided by PosPAC software using Dashmap application from Optech. Dashmap uses the boresighting information from the vehicle and the time stamp of navigation and LiDAR data to provide a geo-referenced point cloud from the surroundings of the vehicle. LiDAR datasets come from the Augas Férreas Square in the city of Lugo, Samil Avenue in the city of Vigo, and Progreso Street in city of Ourense, all these cities located in the Region of Galicia (NW Spain). All the datasets were acquired using normal traffic conditions. Augas Ferreas data comprises 11 strips with a total of 34,352,512 points, Samil Avenue comprises 12 strips with 35,026,765 points, and Progreso Street has 2 strips with 6,181,733 points. The point cloud from Progreso Street is depicted in Fig. 1.

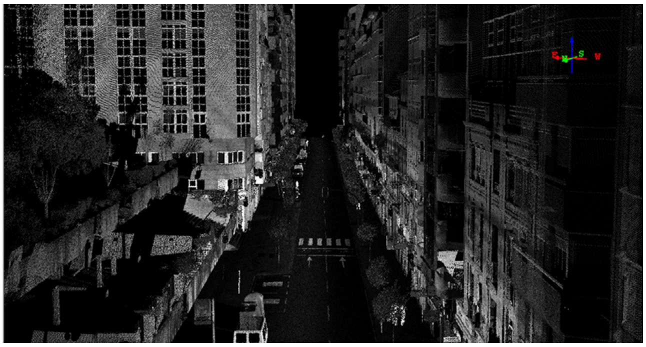

**Fig. 1.** Example of point cloud from Progreso Street in the city of Ourense (Spain).

**Fig. 2.** Optech Lynx mobile mapper. Draw (right) and survey van (left).

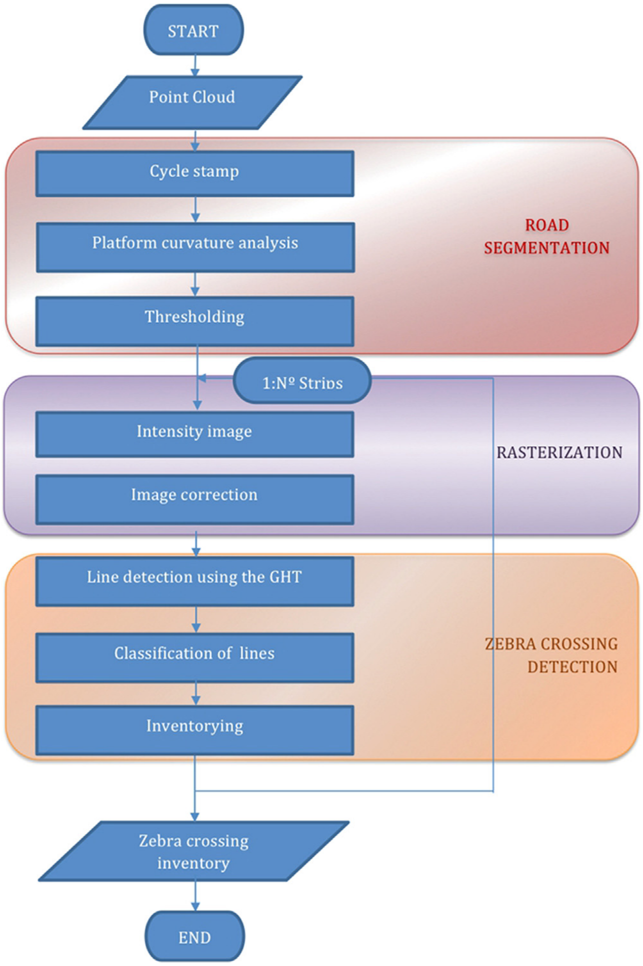

**Fig. 3.** Overall workflow of the algorithm.

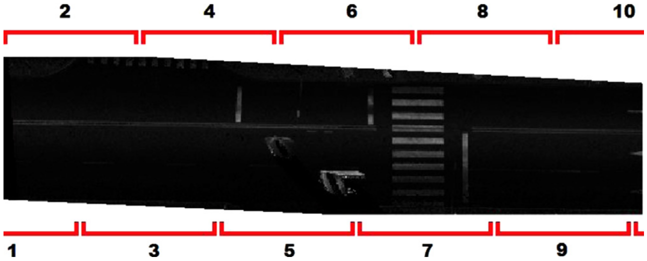

**Fig. 4.** Example of road segmentation and strips with overlap of 50%.

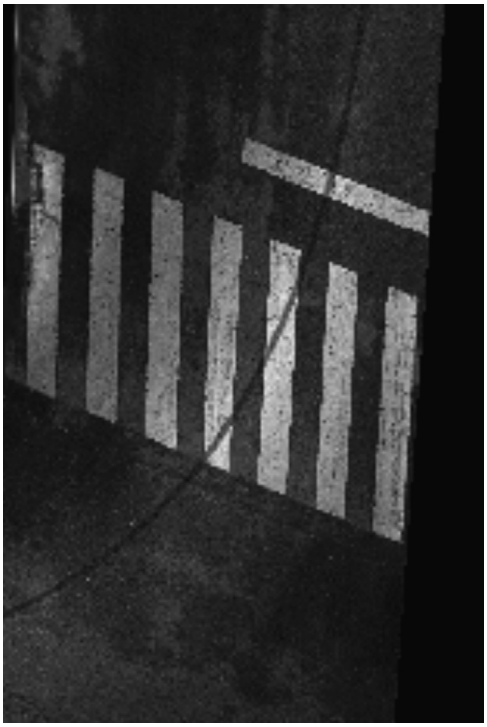

**Fig. 5.** Example of image from zebra crossing obtained using point cloud data. Grayscale image.

### 2.2. Mobile LiDAR system

The mobile LiDAR used for surveying was the Optech Lynx Mobile Mapper (Fig. 2). The mobile LiDAR consists of a navigation system with global navigation and inertial units, two LiDAR sensors, and four digital cameras. All the systems are geometrically boresighted and time stamped to give an accurate and geo-referenced point cloud from the environment after a mobile surveying. The maximum measurement range (according technical specifications from the manufacturer) is 200 m, although according the experience of the authors ranges above 100 m perpendicular to the vehicle are difficult to achieve. Range precision is 8 mm and absolute accuracy 5 cm [17]. PDOP must be lower than 2.5 during the survey to achieve the mentioned absolute accuracy. The laser measurement rate is programmable between 75 and 500 kHz. Intensity of laser light that returns to the detector is recorded in 12 bits form. The system can detect up to 4 returns from each laser pulse. However, in this work only the first return is used. The scan frequency is also programmable between 80 and 200 Hz. The scanner field of view is 360°. This fact provides a complete point cloud in situations as tunnels or overpasses and makes possible the measurement of for example the vertical clearance. It requires a power of 12 VDX and 30 A. Operating temperature ranges between −10 °C and 40 °C.

### 2.3. Data processing algorithm

Algorithm for automatic data extraction of zebra passes position is shown in Fig. 3. Next, the main parts of the algorithm are described.

#### 2.3.1. Road segmentation

The principal component analysis (PCA) is a mathematical procedure that seeks to reduce the dimensionality of a set of variables to a new set of variables (principal components) that are linear combinations of the initial variables and are also uncorrelated to each other. The main components are obtained in decreasing order of importance. It is intended that a number of these, less than the initial number of variables, collect most of the information. The first eigenvector explains the main part of the total variance of the initial data. In this work, a PCA is used in order to detect geometric changes into the

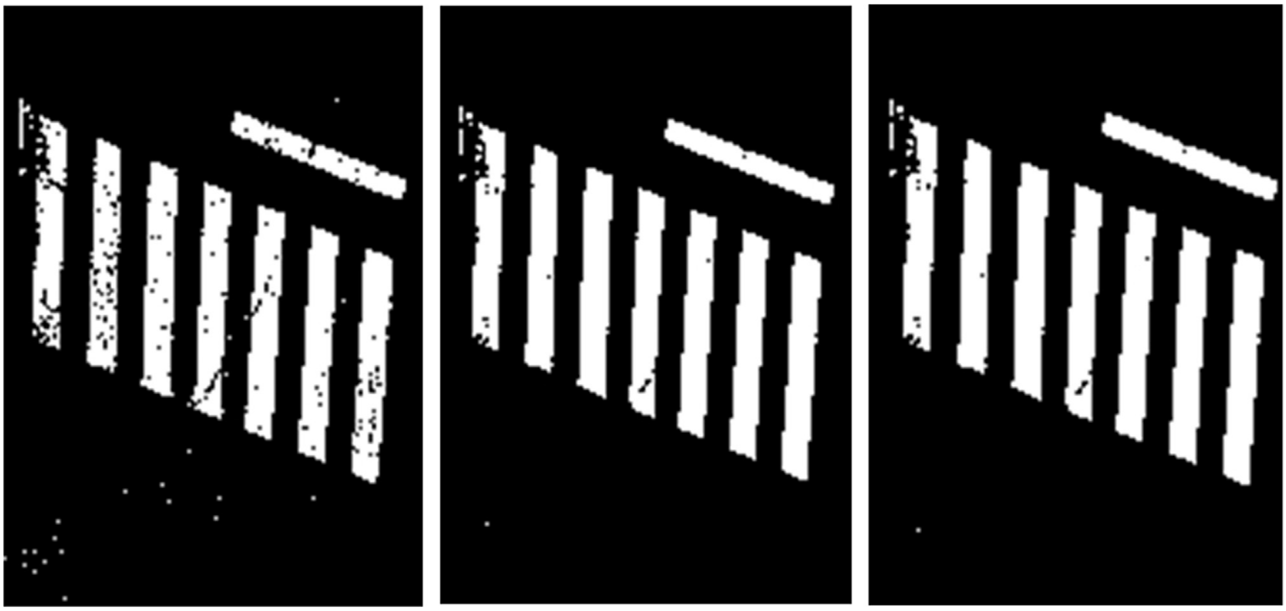

**Fig. 6.** Image binarization from zebra crossing; without median filtering (left), after median filter (center), and after the mathematical morphology operation of closing (right).

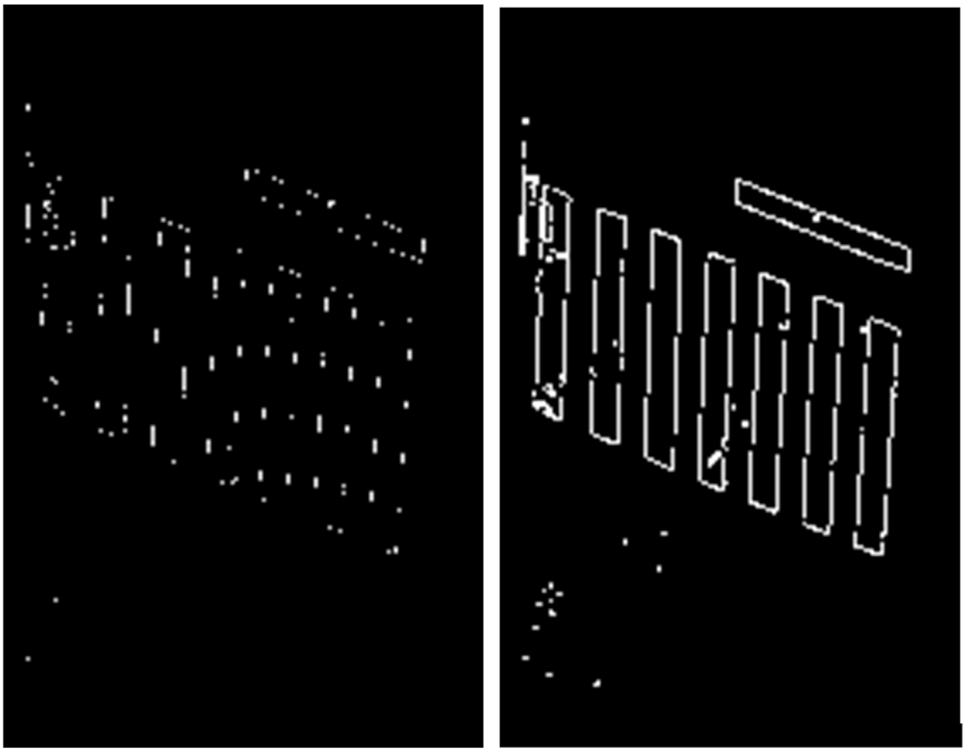

**Fig. 7.** Edge detection of the zebra crossing (left). Image after a dilation (right).

profile defined by the points contained in each scanner cycle [13,18]. Since the data of each cycle is represented into 2D space, analysis is performed using the altitude of each point (Z coordinate) and deflection angle. These two variables allow to easily detect peaks denoting the transversal limits of the road when PCA analysis is performed into the local neighborhood (10 points) of each of the points contained in each scanner cycle.

Once the road is segmented from the rest of the point cloud these down sampled point cloud is partitioned into strips of the same length in order to normalize the data processing. A length of 18 m was established for each strip, which is computed from the navigation data provided by the Optech Lynx Mobile Mapper. An overlap of 50% between adjacent strips is programmed to avoid the loss of relevant information about the urban parts (i.e. zebra crossings). Fig. 4 shows an example of road cutting in strips. For example, the zebra crossing is completely recorded in strip 7. However, if only strips 6 and 8 would be acquired, the data will not provide the complete information from the zebra crossing so the road marking would be hardly detected.

### 2.3.2. Road rasterization

Point cloud data show geometric and radiometric information that can be easily converted in an image to apply image processing algorithms. Image processing techniques are mature and robust, so it is decided to perform this step and convert the LiDAR data to imagery. The radiometric information of each coordinate comes from the reflective intensity of the laser light and depends on the distance between laser emitter and target surface, reflection angle, and target reflectivity. The painted road, as occurs in a zebra crossing, gives high reflectivity in comparison to their surroundings. This characteristic will be used to transform the point cloud data from the road to 2D imaging data.

The first step in road rasterization consists of the projection of the point cloud data on the plane that best fits to the road strip. Next, a

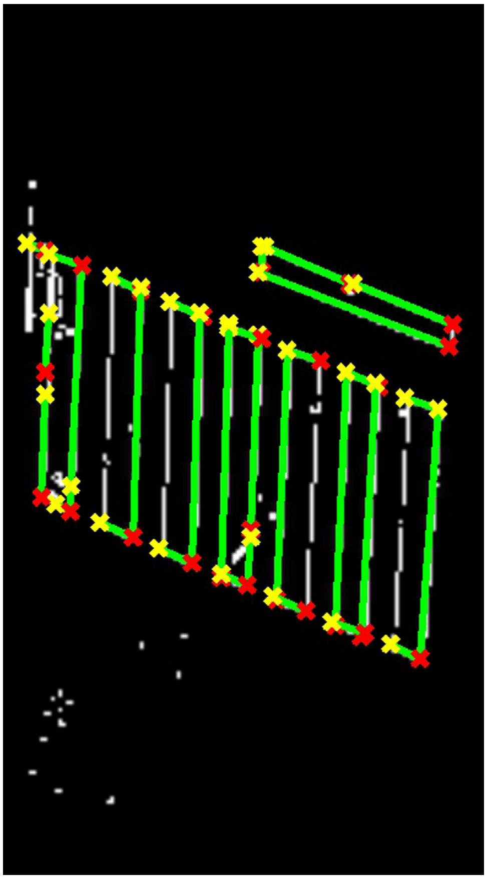

**Fig. 8.** Line detection using the Standard Hough Transform. (For interpretation of the references to color in this figure, the reader is referred to the web version of this article.)

nearest neighbor algorithm is used to assign the intensity data to a regular matrix created on the projection plane. The LiDAR point cloud is a messy system that must be transformed into an array to use image processing techniques. The algorithm calculates the Euclidean distance between each node of the matrix and the neighborhood points. Once the closest point is defined, the value of intensity is assigned to the node [19]. Distance between nodes was selected to be 5 cm to have an enough spatial resolution in the images. Finally, the intensity from the images (12 bits: 0–4095) is normalized between 0 and 1. Fig. 5 shows an example of the rasterized data.

### 2.3.3. *Zebra crossing detection and positioning*

Zebra crossing detection is based in the higher reflectivity of the element and in the characteristic parallel lines of the edges between the painting area and the pavement. Image processing techniques are used in this step of the algorithm [20] in order to ease the detection of the road marks.

The first step consists of the thresholding of the previously normalized image between 0 and 1 from the intensity values of the LiDAR data. The thesholding is calculated using the Otsu method, which chooses the threshold that minimize the intraclass variance of the black and white pixels. An example of binarized image is shown in Fig. 6 (left). Binarization is a fundamental step to divide the image in two basic classes. First class corresponds to the painting area and the second one to the rest of the pavement. The binarization process leaves some small areas with salt and pepper noise. The most common tool to reduce this noise is to apply a median filter (Fig. 6 – center). Fig. 6 (right) shows the results obtained after applying mathematical morphology operations. Particularly a closing operation (dilation followed by and erosion) of the image using a 5 × 5 square structure is performed. The purpose of the closing is to fill the gaps between the pixels in the border of white marks. This morphological operation is critical to achieve robust edge detection.

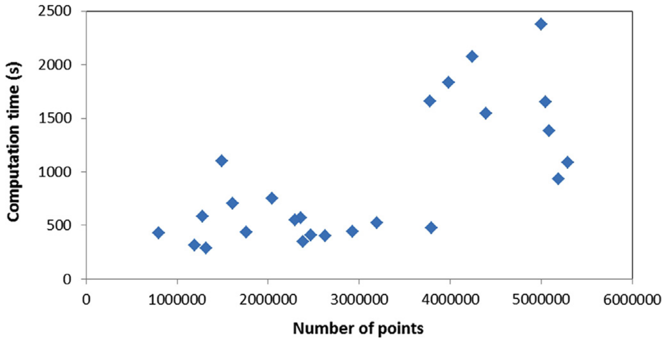

**Fig. 9.** Computation time versus number of points in the cloud.

The second step consists of the edge detection of the zebra crossing. Edge detection is critical to apply then the Standard Hough Transform. Edge detection is performed using the Canny method, which finds edges by looking for local maxima of the gradient of the image. The gradient is calculated using the derivative Gaussian filter. Other methods as Sobel and Prewitt edge detectors were tested; however Canny shows the most reliable results for the type of datasets used in this work. As it can be observed in Fig. 7 (left), edges appear very thin. The tests shown as a thin border inhibits the proper working of the line detector (Standard Hough Transform). Therefore, a dilation operation (Fig. 7 – right) is performed to increase the edge thickness. A 5 × 5 square structure is used for the morphological operation.

The third step is based on the detection of lines in the image using the Standard Hough Transform [21,22]. The Standard Hough Transform is an algorithm employed in pattern recognition, which allows finding shapes as straight lines within the image. Is seems adequate for the purpose of detecting the zebra crossings, since they present a number of straight lines after the edge detection is performed. The operating mode is statistical and uses a parametric representation of the lines. The result of detection is shown in Fig. 8 where the lines detected are depicted in green. To define detection of lines as a zebra crossing the authors establish the criteria that a zebra pass in a common road must be defined by a set of parallel lines with similar

**Table 1**
Algorithm results.

| Site | Strip | Points | Computation time (s) | *X* position (m) | *Y* position (m) | Completeness |
|---|---|---|---|---|---|---|
| Progreso Street | P1 | 3,796,143 | 474 | 593,346 | 4,688,152 | 3/3 |
| | | | | 593,371 | 4,688,086 | |
| | | | | 593,415 | 4,687,972 | |
| | P2 | 2,385,590 | 348 | 593,425 | 4,687,700 | 3/3 |
| | | | | 593,424 | 4,687,855 | |
| | | | | 593,426 | 4,687,759 | |
| Samil Avenue | S1 | 1,756,687 | 438 | 518,695 | 4,674,416 | 1/1 |
| | S2 | 2,359,182 | 570 | 518,841 | 4,674,519 | 1/1 |
| | S3 | 2,467,759 | 411 | 519,038 | 4,674,518 | 1/1 |
| | S4 | 5,290,571 | 1089 | – | – | 0/0 |
| | S5 | 2,929,814 | 443 | 519,210 | 4,674,388 | 1/1 |
| | S6 | 5,193,961 | 932 | 519,445 | 4,674,352 | 1/2 |
| | S7 | 3,197,622 | 524 | – | – | 0/1 |
| | S8 | 2,629,765 | 404 | – | – | 0/0 |
| | S9 | 1,316,111 | 291 | – | – | 0/1 |
| | S10 | 1,610,806 | 707 | 520,138 | 4,673,855 | 1/1 |
| | S11 | 1,188,348 | 315 | – | – | 0/0 |
| | S12 | 5,086,139 | 1385 | 520,391 | 4,673,226 | 1/1 |
| Augas Ferreas Square | A1 | 4,243,692 | 2074 | 618,488 | 4,761,271 | 1/1 |
| | A2 | 5,049,528 | 1652 | 618,549 | 4,761,179 | 1/1 |
| | A3 | 2,294,035 | 550 | 618,644 | 4,761,173 | 1/1 |
| | A4 | 1,279,948 | 581 | 618,343 | 4,761,314 | 1/1 |
| | A5 | 794,258 | 427 | 618,591 | 4,761,444 | 1/1 |
| | A6 | 1,490,190 | 1099 | 618,445 | 4,761,509 | 1/1 |
| | A7 | 3,777,648 | 1657 | 618,345 | 4,761,643 | 1/1 |
| | A8 | 5,000,282 | 2376 | 618,288 | 4,761,578 | 2/2 |
| | A9 | 3,983,655 | 1833 | 618,417 | 4,761,590 | 1/2 |
| | A10 | 2,046,422 | 749 | 618,332 | 4,761,442 | 1/1 |
| | A11 | 4,393,954 | 1541 | 618,235 | 4,761,379 | 1/2 |

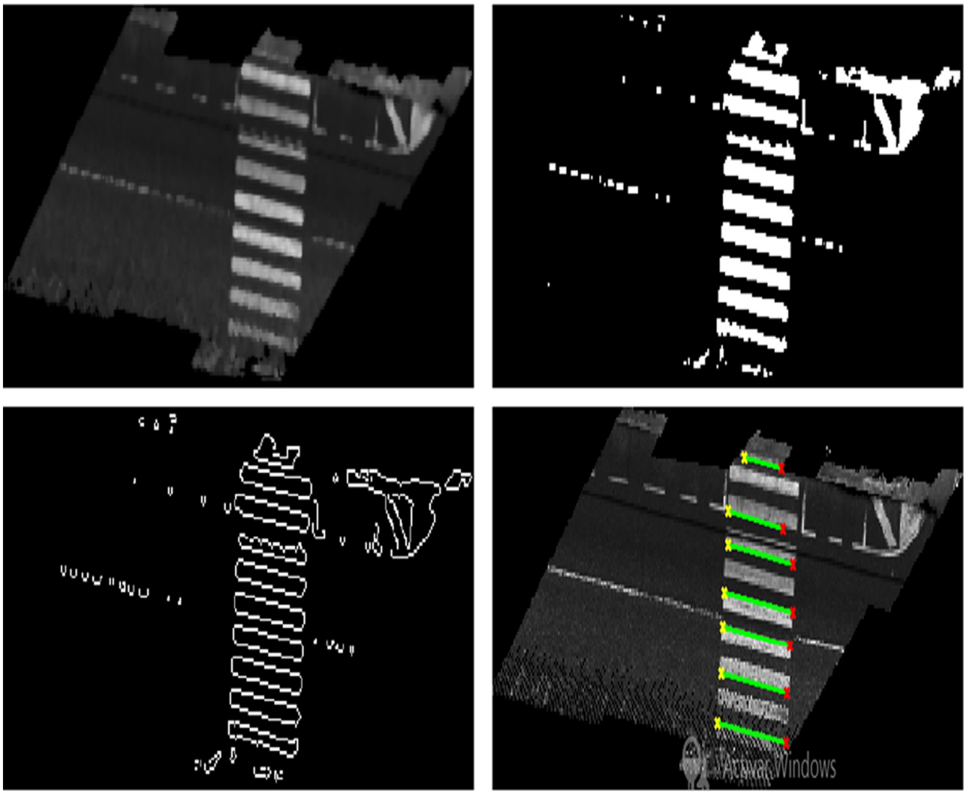

**Fig. 10.** Example of correctly detected zebra crossing in S1. Gray-scale image (top-left), binarized image (top-right), edge detection (bottom-left), and line detection using the Standard Hough Transform (bottom-right).

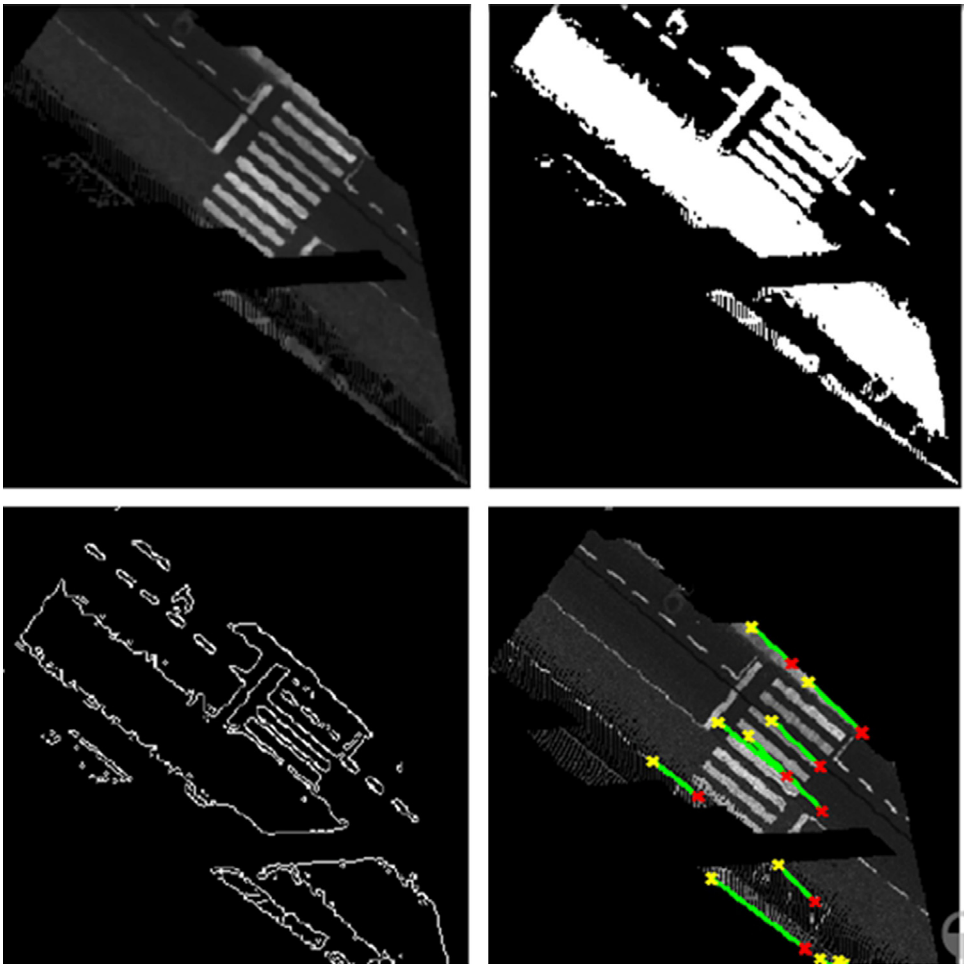

**Fig. 11.** Example of omitted zebra crossing in S6 caused by low intensity gradient between road markings and asphalt. Gray-scale image (top-left), binarized image (top-right), edge detection (bottom-left), and line detection using the Standard Hough Transform (bottom-right).

angle to the direction of the vehicle. The authors establish a limit of 6 lines to avoid false positives. This threshold corresponds to a zebra pass with a minimum of 3 painting areas. The process of checking the number of lines from the Standard Hough Transform detector counting is automatically performed. The global position of the zebra crossing is obtained from averaging the points defining the lines correctly used to identify the road mark from the HT detector. As the pixel coordinates from image come from the point cloud data, the 3D coordinates are directly obtained and the data can be transferred to Geographic Information Systems, for example to perform the inventory of a road. The direction and size of the zebra crossing is computed from the angle defined by lines and their length, respectively.

## 3. Results and discussion

Fig. 9 shows the computation time versus the size of the point cloud. As it must be expected, the computation time increases with the size of the point cloud [23]. Table 1 shows the results obtained from the 3 different study sites. A total of 30 zebra crossings were evaluated with a completeness of 83%. Fig. 10 shows an example of a correctly detected zebra crossing. The results were checked comparing the output of the algorithm with the manual detection performed by a human operator. Some zebra crossing were not detected, although false positives are not presented in the results.

Non-detected zebra crossings are deeply analyzed in order to understand the causes of failure in the algorithm. For example, S6, the largest point cloud under study, shows the omission of one zebra crossing (Fig. 11). The road contains occlusions due to vehicles above the zebra crossing (top-left image). However, in this case these occlusions do not affect negatively to the detection, although in other cases, for example in A10, they can induce a malfunction of the algorithm (Fig. 12). One potential solution to this problem could be to program the survey during the hours when the traffic diminishes (typically at night). In Fig. 11 binarization from the image (top-right) appears slightly deficient, probably by the low reflectivity of the painting of the zebra crossing. This fact diminishes the intensity gradient between the asphalt and the road markings, and decreases

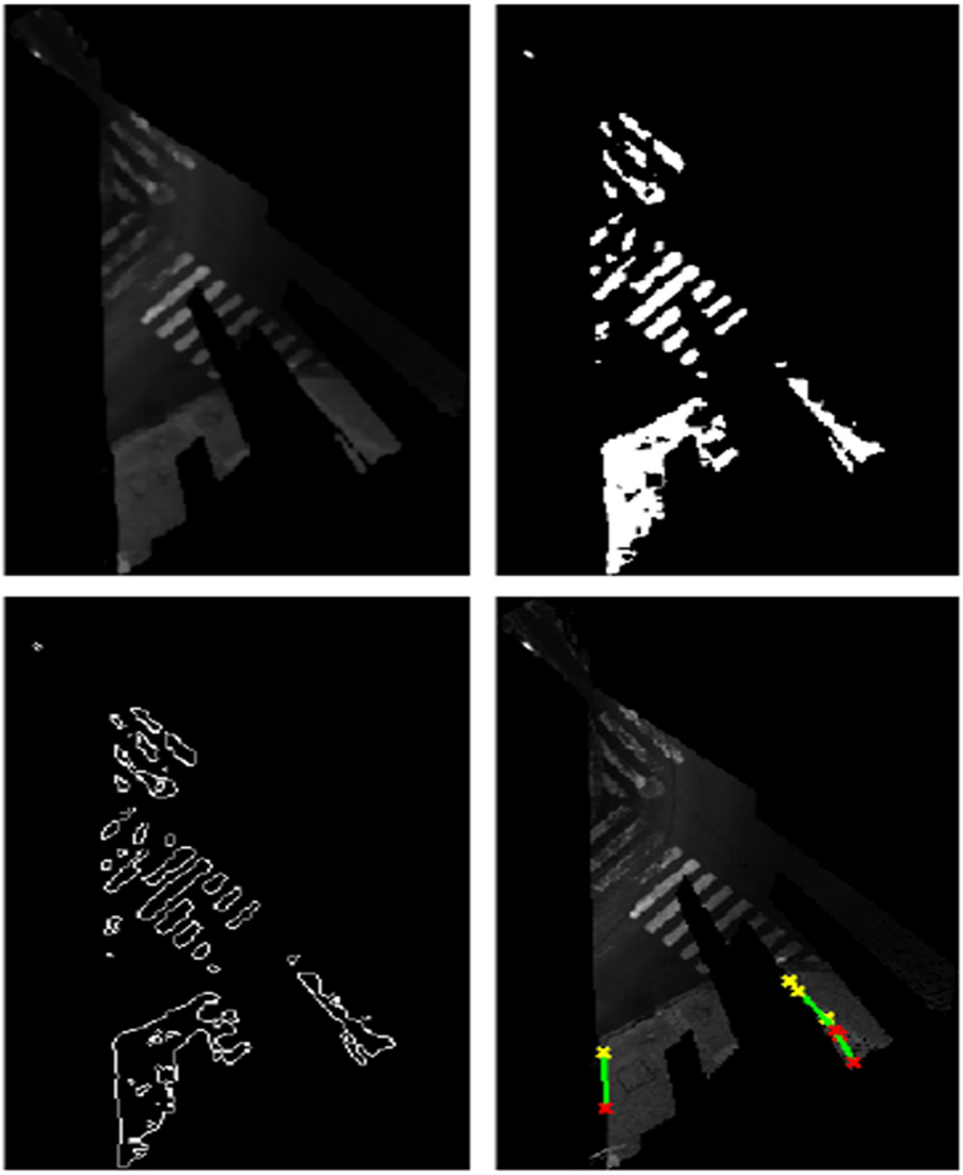

**Fig. 12.** Example of omitted zebra crossing in A10 caused by the occlusions due to vehicles. Gray-scale image (top-left), binarized image (top-right), edge detection (bottom-left), and line detection using the Standard Hough Transform (bottom-right).

the quality of the binarization. It also affects to the edge detection operation (bottom-left) and consequently to the line detection using the Standard Hough Transform (bottom-right).

## 4. Conclusions

An algorithm for the automatic detection of zebra crossing is developed with the aim of automate road inventories using the mobile LiDAR technology.

The algorithm is divided in three main steps: road segmentation, rasterization, and zebra crossing detection. Road segmentation uses the PCA algorithm to perform a curvature analysis and so detect road ends in a LiDAR profile so the point cloud from the road is separated from the rest of the data. In addition the segmented point cloud LiDAR was partitioned into road segments with the same length. Each segment of the road was rasterized, where the digital level is obtained from the intensity of the nearest neighbor point from the cloud, normalized between 0 and 1. Finally, the zebra crossing detection is achieved by using image processing. First, the image is prepared by thresholding of the zebra crossing using the Otsu method, and subsequently median filter of the image, together with mathematical morphology and edge detection algorithms are applied to prepare the data for the object detection. Finally, the Standard Hough Transform is used to detect the parallel lines in the image. The image coordinates of the zebra crossing are obtained by averaging the points provided by the Hough transform. As the image and the point cloud are interconnected the geographic coordinates are obtained.

A completeness of 83% was found when testing the algorithm over 25 strips with 30 zebra crossing. Non-detected zebra crossings were analyzed and the causes of failure principally come from two cases. One consists of the loss of painting of the zebra crossing due to aging, provoking a low intensity gradient between the road and the zebra crossing. The other one comes from the occlusions caused by other vehicles in the point cloud produced during the mobile LiDAR surveying. As expected, computing time increases with the size of the point cloud. It ranges from approximately 2500 s for point clouds over 5 million points to less than 500 s for the smaller point clouds. All the tests were done using Matlab software.

## Acknowledgments

Authors want to give thanks to the Xunta de Galicia (Grant nos. IPP055–EXP44; EM2013/005; CN2012/269) and Spanish Government (Grant nos. TIN2013-46801-C4-4-R; ENE2013-48015-C3-1-R; FPU: AP2010-2969).

## References

[1] Petri G. Mobile mapping systems: an introduction to the technology. Geoinformatics 2010;13(1):32–43.
[2] Puente I, González-Jorge H, Martínez-Sánchez J, Arias P. Review of mobile mapping and surveying technologies. Measurement 2013;46(7):2127–45.
[3] Graham L. Mapping systems overview. Photogramm Eng Remote Sens 2010;76 (3):222–8.
[4] Jaakkola A, Hyyppa J, Kukkp A. Retrieval algorithms for road surface modeling using laser-based mobile mapping. Sensors 2008;8(9):5238–49.
[5] Hernandez J, Marcotegui B. Filtering artifacts and pavement segmentation from mobile LiDAR data. Laser scanning – IAPRS 2009: XXXVIII (Part3/W8); 2009. p. 329–33.
[6] Pu S, Rutzinger M, Vosselman G, Oude ES. Recognizing basic structures from mobile laser scanning data for road inventory studies. ISPRS J Photogramm Remote Sens 2011;66(6):S28–39.
[7] Mc Elhinney C, Kumar P, Cahalane C, Mc Carthy T. Initial results from the European road safety inspections (EURSI) mobile mapping project. Int Arch Photogramm Remote Sens Spat Inf Sci 2010;XXXVII(Part 5):440–5.
[8] Kumar P, McElhinney CP, Lewis P, McCarthy T. An automated algorithm for extracting road edges from terrestrial mobile LiDAR data. Remote Sens 2013;85:44–55.
[9] Puente I, González-Jorge H, Martínez-Sánchez J, Arias P. Automatic detection of road tunnel luminaires using a mobile LiDAR system. Measurement 2014;47:569–75.
[10] Wang J, González-Jorge H, Lindenbergh R, Arias-Sanchez P, Menenti M. Automatic estimation of excavation volume from laser mobile mapping data for mountain road widening. Remote Sens 2013;5:4629–51.
[11] Cabo C, Ordoñez C, García-Cortés S, Martínez J. An algorithm for automatic detection of pole-like Street furniture object from mobile laser scanner point clouds. ISPRS J Photogramm Remote Sens 2014;87:47–56.
[12] González-Jorge H, Puente I, Riveiro B, Martínez-Sánchez J, Arias P. Automatic segmentation of road overpasses and detection of mortar efflorescence using mobile LiDAR data. Opt Laser Technol 2013;54:353–61.
[13] Holgado-Barco A, González-Aguilera D, Arias-Sánchez P, Martínez-Sánchez J. An automated approach to vertical road characterization using mobile LiDAR systems: longitudinal profiles and cross-sections. ISPRS J Photogramm Remote Sens 2014;96:28–37.
[14] Lausser L, Schwenker F, Pal, G. Detecting zebra crossings utilizing AdaBoost. In: Proceedings of the European symposium on artificial neural networks – advances in computational intelligence and learning; 2008. p. 535–40.
[15] Boudet L, Midenet S. Pedestrian crossing detection based on evidential fusion of video-sensors. Transp Res C 2009;17(5):484–97.
[16] Broggi A, Cerri P, Ghidoni S, Grislei P, Jung HG. A new approach to urban pedestrian detection for automatic braking. IEEE Trans Intell Transp Syst 2009;14(3):594–605.
[17] Puente I, González-Jorge H, Riveiro B, Arias P. Accuracy verification of the Lynx Mobile Mapper system. Opt Laser Technol 2013;45:578–86.
[18] Díaz-Vilariño L, Lagüela S, Armesto J, Arias P. Semantic as-built 3d models including shades for the evaluation of solar influence on buildings. Sol Energy 2013;92:269–79.
[19] Bolstad P. GIS fundamentals. 4th ed.. Fayetteville, North Carolina, USA: Publisher Atlas Books; 2008.
[20] González R, Woods R. Digital image processing. 3rd ed.. Upper Saddle River, New Jersey, USA: Publisher Prentice Hall; 2007.
[21] Hough PVC. Methods and means for recognizing complex patters. US patent 3069654; 1962.
[22] Ballard DH. Generalizing the Hough Transform to detect arbitrary shapes. Pattern Recognit 1981;13(2):111–22.
[23] Varela-González M, González-Jorge H, Riveiro B, Arias P. Performance testing of LiDAR exploitation software. Comput Geosci 2013;54:122–9.